PON1 Deficiency Promotes TREM2 Pathway-Mediated Microglial Phagocytosis and Inhibits Pro-Inflammatory Cytokines Release in Vitro and in Vivo

Li Zhang
ILAS: Chinese Academy of Medical Sciences Institute of Laboratory Animal Sciences
Wei Dong
ILAS: Chinese Academy of Medical Sciences Institute of Laboratory Animal Sciences
Yuanwu Ma
CAMS ILAS: Chinese Academy of Medical Sciences Institute of Laboratory Animal Sciences
Lin Bai
CAMS ILAS: Chinese Academy of Medical Sciences Institute of Laboratory Animal Sciences
Xu Zhang
CAMS ILAS: Chinese Academy of Medical Sciences Institute of Laboratory Animal Sciences
Caixian Sun
CAMS ILAS: Chinese Academy of Medical Sciences Institute of Laboratory Animal Sciences
Jingwen Li
CAMS ILAS: Chinese Academy of Medical Sciences Institute of Laboratory Animal Sciences
lianfeng zhang (zhanglf@cnilas.org)
Chinese Academy of Medical Sciences Institute of Laboratory Animal Sciences https://orcid.org/0000-0002-5774-2924

Research Article

Keywords: PON1, microglia, TREM2, interaction, knockout rats, phagocytosis, Aβ, LPS

Posted Date: August 23rd, 2021

DOI: https://doi.org/10.21203/rs.3.rs-673247/v2

Abstract

Paraoxonase 1 (PON1) plays an anti-inflammatory role in the cardiovascular system. Levels of serum PON1 and polymorphisms in this gene were linked to Alzheimer disease (AD) and Parkinson disease (PD), but its function in the neuroimmune system and AD are not clear. To address this issue, we used PON1 knockout rats previously generated by our lab to investigate the role of PON1 in microglia. Knockout of PON1 in rat brain tissues protected against LPS-induced microglia activation. PON1 deficiency in rat primary microglia increased TREM2 (triggering receptor expressed in myeloid cells 2) expression, phagocytosis and IL-10 (M2-phenotype marker) release, but decreased production of pro-inflammatory cytokines such as IL-1β, IL-6, IL-12, IL-18 especially TNF-α (M1-phenotype markers) induced by LPS. PON1 deficiency in rat primary microglia activated TREM2 pathway but decreased LPS-induced ERK activation. The phagocytosis promoting effect of PON1 knockout could be reversed by administration of recombinant PON1 protein. The interaction between PON1 and TREM2 was verified by co-immunoprecipitation (co-IP) using rat brain tissues or over-expressed BV2 cell lysates, which might be involved in lysosomal degradation of TREM2. Furthermore, PON1 knockout may also enhance microglial phagocytosis and clearance of exogenous Aβ by an intrahippocampal injection and decrease the transcription of cytokines such as IL-1β, IL-6 and TNF-α in vivo. These results suggest an inhibitory role of PON1 in microglial phagocytosis dependent on its interaction with TREM2. These findings provide novel insights into the role of PON1 in neuroinflammation and highlight TREM2 as a potential target for Alzheimer's disease therapy.

Background

PON1 is a member of the multi-gene paraoxonase (PON) family comprised of three members, PON1, PON2 and PON3, located on chromosome 7 in humans [1]. Human PON1 is an esterase that displays both paraoxonase and arylesterase activities for hydrolyzing and detoxifying toxic organophosphorus compounds, interaction with various drugs, and antioxidant activity by hydrolyzing oxidized phospholipids in high-density lipoprotein (HDL) and low-density lipoprotein (LDL) [2-6]. PON1 expression can be modulated by diet, life-style and pharmaceuticals [7], but also by genetic polymorphisms in the promoter and coding regions [8-10]. PON1 is now considered to be a major antioxidant factor for eliminating oxidized HDL [5]. Levels of serum PON1 and polymorphisms in the PON1 gene were linked to atherosclerosis, coronary artery disease, and stroke [11-14].

PON1 is synthesized mainly in the liver and secreted into the blood where it associates predominantly with HDL [2]. However, immunohistochemical studies and RT-PCR have revealed the presence of PON1 in a wide variety of tissues including brain, spinal cord, heart and kidney in humans [15], mice [16] and rats [17]. Whether this is due to local synthesis or to PON1 being transported from liver to other tissues by HDL is unclear. Although PON1 is present in brain tissue, its role in neurodegenerative diseases is controversial. Many studies on Parkinson's disease (PD) suggest that the MM55 PON1 genotype is a susceptibility marker for PD and is associated with exposure to organophosphates in the environment [18]. Neither L55M nor Q192R PON1 show association with the pathogenesis of PD,

however [19]. In dementias, associations with beta-amyloid levels, senile plaque accumulation and cholinesterase activity suggest an involvement of the PON1 gene in the pathogenesis of AD and response to treatment [20]. AD and other dementias are associated with decreased PON1 activity [21, 22], but the majority of meta-analyses failed to find any association between PON1 polymorphisms and the development of neurodegenerative diseases such as AD and PD [23, 24]. PON1 might be a potential player in the pathogenesis of neurological disorders, but the precise pathogenic links and the mechanisms are still unclear.

In previous studies, we established a PON1 knockout (KO) rat model and found that PON1 KO impaired T cell development in the thymus [25], suggesting that PON1 might be a novel immune regulator. As the resident macrophages of the central nervous system (CNS), microglia strongly influence the pathological response to a stressor by cordoning off brain lesions, phagocytizing cellular debris, and releasing cytokines, chemokines, and growth factors [26, 27]. However, the role of PON1 in microglial phagocytosis is unknown. In the present study, we demonstrated that PON1 inhibited microglial phagocytosis by down-regulation of triggering receptor expressed in myeloid cells 2 (TREM2). Knockout of PON1 negatively regulated the production of pro-inflammatory cytokines induced by LPS or Aβ but facilitated TREM2-dependent microglial phagocytosis in vivo and in vitro.

Methods

Human brain samples and animals

Human brain tissues were obtained from the Human Brain Bank as previously described [28]. PON1$^{-/-}$ rats were generated previously in our lab [25]. Knockout (KO) rats were genotyped by PCR using the primers, 5' AAGCGGGTGCTGAAGACT and 5 'ACTGCTGGCTCCTTCTCA. A 521-bp fragment of WT and a 179-bp fragment of the PON1 KO gene were amplified with 30 PCR cycles consisting of 94°C for 30 s, 60°C for 30 s and 72°C for 45 s. All rat experiments were approved by the Animal Care and Use Committees of the Institute of Laboratory Animal Science of Peking Union Medical College (ZLF18002).

LPS administration

WT and PON1$^{-/-}$ rats have similar body weight at the same age (Fig.S2). PON1 KO rats (250-300 g) and control SD rats (250-300 g) were given an intraperitoneal injection of saline (control) or 5 or 20 mg/kg LPS (Sigma).

Survival Analysis

The cumulative percent mortality was calculated every 12 hours for LPS-treated rats during the 48-h period after injection. Survival was determined at the point where no further loss of animals occurred. Kaplan-Meier curves were generated using GraphPad Prism 7.

Histochemical staining and analysis

Rats were anaesthetized with pentobarbital and the brains were carefully dissected out. Routinely, brain tissues were fixed in 10% formalin andembedded in paraffin blocks. After heat mediated antigen retrieval with Tris/EDTA buffer pH 9.0 were performed, sections were stained with antibody to the microglia marker, ionized calcium-binding adaptor protein-1 (Iba1) (1:200, ab178847, abcam). Stained sections were scanned using a Panoramic III scanner (3D Histech, Hungary) and digital images were obtained. Images were analyzed using Image J software according to the protocol reported previously by Young and Morrison[29]. The sections were evaluated by an observer blinded to the rat genotypes.

Serum

At the indicated time points after LPS injection, blood samples were taken and allowed to clot for 30 min at room temperature. Serum was obtained after centrifugation at 1500×g for 10 min at 4 °C.

Cell culture and treatment

Microglial cells were isolated from brains of 1-3 day-old neonatal WT or PON1$^{-/-}$rats according to a previously described procedure with modifications [30]. Briefly, after enzymatic digestion and mechanical dissociation, mixed glial suspensions were filtered through a 70-μm cell strainer, and cells were collected by centrifugation, resuspended in DMEM/F12 supplemented with 10% FBS (Gibco), and cultured in 75-cm^2 flasks (Nunc, Roskilde, Denmark) in a humidified atmosphere of 5% CO_2 /95% air at 37°C. After 7-10 days, the top layer microglia cells were obtained by shaking off the astrocytic layer of the glial cultures and harvested by centrifugation and seeded onto 6 or 12-well plates for further experiments. Microglia were treated with LPS (Sigma) at a concentration of 200 ng/mL or recombinant human PON1 protein (TP310356, Origene). Control cells were treated with DPBS. Cells for immunofluorescence analysis were seeded onto glass coverslips in 12 -well plates. Cells for RT-PCR and western blot were seeded onto 6 -well plates.

BV2, a mouse microglial cell line, was cultured in DMEM containing 10% FBS (Gibco) with 1% penicillin/streptomycin (Invitrogen). For co-IP and western blot, BV2 cells were seeded onto 10-cm culture dishes and harvested 36-48h following transfection.

Cytokine and chemokine measurement

Rat serum was collected and the level of IL-10 and TNF-α in serum was determined using ELISA kits (R1000 and RTA00, R&D Systems). Cell culture supernatants were obtained by centrifugation and cytokines were detected with a 23-plex rat cytokine panel (Luminex).

Western immunoblotting

Total protein lysates from rat brain tissues or cultured cells were prepared as previously described [28]. After SDS-PAGE, the proteins were transferred to nitrocellulose (Millipore), and the membranes were incubated overnight with antibodies against PON1 (1:500, ab24261, abcam) (Antibody against p-DAP12 was designed and prepared by Genscript in USA, and other antibodies used are listed in **Table S1**). After

incubation with the appropriate secondary antibody for 1h at room temperature, antibody binding was detected with an HRP-conjugated immunoglobulin G (Santa Cruz) using a chemiluminescence detection system (Santa Cruz). For quantitative analysis, the PON1 level was normalized to GAPDH using Image J software.

RNA isolation and quantitative RT-PCR

Total RNA was extracted using Trizol (Invitrogen, UK) and treated with RNase-free DNase I to remove any contaminating genomic DNA. First-strand cDNA was synthesized from 2 ug of total RNA using random hexamer primers according to the Superscript III reverse transcriptase manufacturer's protocol (Invitrogen, USA). Detection of PON1 and TREM2 mRNA was carried out by RT-PCR, using GAPDH for normalization. The primers for human PON1 were 5'- TTGGGTTTAGCGTGGTCGTAT-3' and 5'-TCCAACCCAAAGGTCTCCTG -3'; for human GAPDH 5'- AACGGATTTGGTCGTATTG-3' and 5'-GCTCCTGGAAGATGGTGAT'. The primers for rat PON1 were 5'-TAAAGGAATCGAAGCGGGTGC-3' and 5'-CGGTGGACGAGGAGTCTGG-3'; for rat GAPDH 5'- TATCGGACGCCTGGTTAC-3' and 5'-TGCTGACAATCTTGAGGGA-3'. For rat TREM2: r-TREM2-F 5'-CTCTCCACGTGTTTGTCCTGT-3'; r- TREM2-R 5'-TCATCTGTGATGACCGTGCT-3'. The primer sequences of seven cytokines were listed in supporting Table S2. Twenty-four cycles of RT-PCR were performed using the following conditions: denaturation at 94°C for 30 s; annealing for rat or human PON1 and TREM2 at 60°C for 30 s; annealing at 55°C for GAPDH for 30 s; and extension at 72°C for 30 s.

RNA sequencing

RNA sequencing was done by Novogene (Beijing, China). Briefly, total RNA was isolated from rat primary microglia treated with or without LPS and RNA-Seq libraries were prepared by standard protocols. After cluster generation, the libraries were sequenced on an Illumina Hiseq platform and 125 bp/150 bp paired-end reads were generated. Differential gene expression analysis was performed using the DESeq2 R package (1.16.1). The *p* values were adjusted using the Benjamini & Hochberg method and $p<0.01$ was the criterion for differential expression. Gene ontology (GO) enrichment analysis was performed by function 'sota' in the 'clValid' package and GO terms with $p< 0.01$ were considered significantly enriched by differential expressed genes.

Immunofluorescence

Primary microglia were seeded on coverslips overnight and then fixed using 4% paraformaldehyde. Immunofluorescence staining was performed post-fixation using the antibodies listed in **Table S1** and appropriate secondary antibodies. Images were captured using a laser scanning confocal microscope (SPF Leica) and processed with Photoshop version 7 (Adobe Systems Inc.).

Co-immunoprecipitation (co-IP) assays

To determine the interaction between PON1 and TREM2, co-IP assays for both proteins from gene-transfected cells and endogenous proteins were performed.

For gene-transfected co-IP assay, BV2 cells seeded in 10 cm dishes were transiently cotransfected with 5 μg of Myc-PON1(HG13083-CM, Sino Biological) and 5 μg of Flag-TREM2 (HG11084-CF, Sino Biological) or 5 μg of Myc-TREM2 (HG11084-CM, Sino Biological) and 5 μg of Flag-PON1 (HG13083-CF, Sino Biological), using the FuGENE® HD transfection reagent (E2311, Promega) according to manufacturer's instructions. As a control, Myc-PON1 or Myc-TREM2 and 5 μg of empty vector pCMV3 were co-transfected in parallel. At 24-36 h post-transfection, cells were harvested and lysed with Pierce IP Lysis buffer (Thermo) containing protease inhibitors (Roche), and cell lysates were incubated with anti-flag M2 affinity gel (A2220, Sigma) overnight at 4°C. The precipitates were collected by centrifugation, washed with ice-cold phosphate-buffered saline (PBS) three times, eluted with 60 μL of SDS loading buffer, and subjected to western blot analysis.

For endogenous proteins, total brain lysates were prepared with the same IP buffer as above. One aliquot was used for IP of the target protein, while the other served as the input control. PON1 antibody (1:100, ab126597, abcam)was added to the lysate and incubated overnight at 4°C on a tube roller-mixer at low speed. The following day, 50 μL of protein A/G agarose (Pierce 20241, Thermo) was added to the lysates and incubated at room temperature for two hours. The precipitates were collected and analyzed as above.

Phagocytosis

Microglial phagocytosis of TAMRA labeled beta-amyloid (AS-60488, 1 mM, Anaspec) and FITC-dextran (53557-1G, 1 mg/ml, Sigma) was quantified by confocal microscopy after incubation of microglial cells at 37°C. At the indicated time points, the Aβ- or dextran-containing medium was removed and cells were washed, fixed with 4% PFA, and incubated with DAPI (Thermo Fisher) for staining the nuclei.

Disuccinimidyl suberate (DSS) crosslinking

Binding of PON1 and APOE was examined by cross-linking. The crosslinking reagent disuccinimidyl suberate (DSS) was added at a concentration of 5 mM to mechanically fractured rat brain tissues. After 30 min at room temperature, a quench solution was added to a final concentration of 20 mM Tris (pH 7.5) and incubated for 15 minutes at room temperature. SDS-sample buffer was added to the reaction mixture and heated at 90°C for 5 min. Western blots were exposed to the corresponding antibodies for the detection of PON1, APOE and TREM2 (**Table S1**).

Stereotactic injections

Before Aβ1-42 (ChinaPeptides，Shanghai) was used, it was firstly incubated in sterile saline at 37°C for 2 days to allow the formation of different-sized oligomers. Three-month old WT and PON1-/- rats, weighing 250–300 g, were randomly divided into four groups: 0-day, 3-day, 7-day model, and 14-day model. The rats were anesthetized and maintained with 1.5%-2% isoflurane in oxygen, mounted in a stereotactic frame (RWD, Shenzhen, China), and injected with 4ug/1ul Aβ1-42 into each side of the hippocampus at coordinates (AP: −3.5 mm, ML: 2.0 mm, DV: 3.0 mm) using a Nanoliter injector 2000 (World Precision

Instruments Inc., Sarasota, FL, USA). The injection was performed within 5 min and following the injection, the needle remained in the target location for 5 min before it was gradually withdrawn.

Statistical analyses

All experiments were performed at least three times, and all samples were tested in triplicate. The data are shown as the mean± S.D. unless otherwise noted. Student's *t*-test was used for statistical analysis when only two groups were tested. Two-way analysis of variance was used to compare multiple groups. In all cases, a $p< 0.05$ was considered statistically significant. Statistical analyses were performed using Graph Pad Prism version 7.0 (Graph Pad Software, La Jolla, CA, USA).

Results

PON1 is expressed in both human and rat brain tissues and rat primary microglia.

Given the important function of PON1 in macrophages [31], we proposed that PON1 might play a role in brain macrophages, microglia. PON1 mRNA was detected in both human and rat brain tissues and the level in rat liver was approximately 3.8 times higher than in rat brain (**Fig. 1A, B**). The absence of PON1 protein in PON1 KO rats was confirmed by western blot of total proteins from brain tissues and primary microglia (**Fig. 1C, D**). PON1 was also detected in HM1900 and BV2 microglia cell lines (**Fig. S1**). To identify the location of PON1 protein in microglia, we stained brain tissue sections from WT rats at two months of age. Immunofluorescence analysis indicated that PON1 protein was primarily localized in neurons, but also expressed in a small number of Iba1-positive microglia (**Fig. 1E**). Unlike the results from brain tissue sections, immunofluorescence staining of primary microglia from neonatal rats showed PON1 co-localized with Iba1 in almost all microglia. PON1 immunostaining was not observed in microglia from PON1$^{-/-}$ rat (**Fig. 1F**). PON1 also co-localized with MAP2 in cultured neurons and with GFAP in cultured astrocytes (**Fig. 1G**).

PON1 deficiency reduces LPS lethality

Exposure to bacterial lipopolysaccharide (LPS) induces tumor necrosis factor (TNF-α) production and causes death in rodents [32-34]. Intravenous injection of 20 mg/kg LPS into WT rats resulted in death of 100% (5/5, female) of the rats within 48 h after injection. In contrast, only 40% of the PON1$^{-/-}$ (2/5, female) rats were dead within 48 h at the same dose. Intravenous injection of 5 mg/kg LPS into WT rats resulted in death of 26.7% (4/15) of the rats within 48 h. In contrast, just 6.7% (1/15) of PON1$^{-/-}$ rats was dead within 48 h after injection of 5 mg/kg LPS. This significant ($p<0.05$) difference in LPS mortality demonstrates that PON1 deficiency protects against LPS-induced death (**Fig. 2A**). The appearance of WT and PON1$^{-/-}$ rats at 1 h and 6 h after injection of 5 mg/kg LPS is shown in **Fig. 2B**.

TNF-α is considered to be the cytokine responsible for LPS lethality. Inhibition of the LPS-induced serum levels of TNF-α by the absence of PON1 is expected to make rats less susceptible to LPS. The level of TNF-α in the peripheral blood of PON1-/- rats ($n = 4$) and WT rats ($n = 4$) was determined up to 3 h after

injection of a lethal dose of LPS (20 mg/kg) and the results indicated that both WT and KO rats showed an increase in TNF-α starting at 30 min after injection, peaking at 90 min and declining between 120 and 180 min (**Fig. 2C**). TNF-α levels in PON1$^{-/-}$ rats declined significantly faster than in WT rats (p <0.01, two way ANOVA), indicating that the absence of PON1 protects against the toxic effects of LPS in rats. An ELISA was also performed and confirmed that the absence of PON1 decreased TNF-α (**Fig. 2D**, p <0.05 n = 4/group) and increased the release of IL-10 (**Fig. 2E**, p <0.05, n = 4/group) in serum at 6 h after injection of 5 mg/kg LPS.

PON1 deficiency inhibits LPS-induced microglial activation in vivo

PON1 inhibits monocyte-to-macrophage differentiation and PON1 KO caused obvious morphological changes of macrophages in mice [35]. The results of Iba1 immunohistochemistry showed that the microglia in brain sections from PON1$^{-/-}$ rats were larger (**Fig. 3A-C**) and had fewer and shorter branches (**Fig. 3D, E**) than those from WT rats without LPS treatment. The microglia from WT rats with LPS treatment showed M1-like activation and polarization with amoeboid shape with no long branches (**Fig. 3A, B**). In contrast, the microglia from PON1$^{-/-}$ rats still had large cell bodies with several longer branches than those from WT rats after LPS stimulation.

PON1 deficiency in rat microglia decreased LPS-induced cytokine levels

The phenotypes of primary microglia were further analyzed by immunofluorescence staining and cytokine measurement. The microglial cells from PON1$^{-/-}$ rats were larger than those from WT rats and LPS treatment decreased the cell size in WT rats but not those in PON1$^{-/-}$ rats (**Fig. 4A**). To determine whether PON1 KO altered cytokine release from microglia, we quantified the levels of IL-1β, IL-6, IL-12, IL-18, TNF-α (M1-phenotype markers) and IL-10 (M2-phenotype marker) in cell supernatants following LPS administration (**Fig. 4B**). IL-1β, IL-6, and TNF-α were all significantly decreased (48.4%, 17.1% and 26.6% respectively) in PON1$^{-/-}$ microglia compared to WT. A significant 4.5-fold increase of IL-10 was observed in PON1$^{-/-}$ microglia compared to WT. The increase in LPS-induced M1-phenotype markers, IL-12, IL-18 and TNF-α was smaller in PON1$^{-/-}$ microglia than in WT; although IL-1β, IL-6, IL-12, IL-18, TNF-α, and IL-10 were all increased in WT and PON1$^{-/-}$ microglia after LPS. The increase in LPS-induced IL-10 (M2-phenotype marker) in PON1$^{-/-}$ microglia was larger than in WT. Additional seven cytokines of IL-4, IL-5, IL-7, IL-12, MCP-1, VEGF and G-CSF showed no significant difference between the two groups (**Fig.S3**). IL-4VInducible nitric oxide synthase (iNOS), a key inflammatory mediator, was also significantly increased in WT and PON1$^{-/-}$ microglia after LPS stimulation; but the increase of iNOS in PON1$^{-/-}$ microglia was smaller (**Fig.4C, D**). In accord with the cytokine results, the increase in P-ERK/ERK in PON1$^{-/-}$ microglia was less than in WT (**Fig.4E**), which might explain the differences in cytokine release. These data also suggest that PON1 KO promotes M2-Like polarization in rat microglia.

PON1 deficiency enhances phagocytosis in rat primary microglia

To determine whether PON1 deficiency affected phagocytosis, we measured the internalization of fluorescently labeled Aβ peptide, previously reported to be phagocytosed by microglia [36]. The results demonstrated that PON1 depletion significantly enhanced intracellular levels of fluorescent Aβ (**Fig. 5A, B**). Consistent with the enhanced uptake, we found a similar effect using fluorescently labeled dextran (**Fig. 5C, D**), which targets phagocytosed compounds. These results show that PON1 depletion in microglia increased the overall phagocytic activity. A 24 h treatment with 200 ng/ml LPS inhibited the phagocytic ability of WT and PON1-depleted microglia (**Fig. 5A-D**). Addition of human recombinant PON1 protein to WT and PON1$^{-/-}$ microglia inhibited the phagocytic ability of both (**Fig. 5E, F**).

PON1 deficiency and LPS treatment changed the transcriptomic profiles in rat primary microglia

Twelve microglia samples treated with or without LPS (200 ng/ml) were subjected to RNA-seq. Differential expression analysis demonstrated that PON1 knockout down-regulated a number of genes associated with nervous system development, cell-cell signaling, glial cell differentiation and gliogenesis, while only two genes associated with nervous system development were up-regulated **(Fig. 6A, B, Table 1)**. However, after LPS treatment, PON1 knockout microglia showed an increase in down-regulated and up-regulated genes associated with nervous system development and regulation of ion transport (**Fig. 6 A, C, Table 1**). LPS treatment resulted in similar changes in gene profile in PON1 KO and WT rats (**Fig. 6D-G**, fold change >2, p <0.01). The genes with the most significant variation were classified in four categories by GO analysis. The two categories of up-regulated genes induced by LPS treatment were associated with the defense response, the response to lipopolysaccharide, the response to molecule of bacterial origin, immune system processes and multi-organism processes (**Fig. 6D, E**, p <0.01). Additional categories of down-regulated genes induced by LPS treatment were associated with immune system processes, the dynein complex, leukocyte differentiation, extracellular matrix, chromosome segregation and the proteinaceous extracellular matrix (**Fig. 6F, G**, p <0.01). These results demonstrate that PON1 KO changed the transcriptome profiles of microglia, which might be partly responsible for the phenotypic changes of microglia from PON1 KO rats.

PON1 deficiency up-regulated TREM2 signal in rat primary microglia

To investigate the mechanism underlying PON1-mediated phagocytosis and cytokine release, we analyzed the protein expression of genes that are known to be involved in LPS response and phagocytosis (**Fig.7, Fig.S4, Fig.S5**). Triggering receptor expressed on myeloid cells 2 (TREM2) is a receptor expressed in microglia. The TREM2/DAP12 signaling pathway reduces inflammatory responses and promotes phagocytosis. As expected, TREM2 (**Fig. 7A, B**) and the phosphorylated tyrosine kinase, P-Syk, (**Fig. 7A, C**) were significantly increased in PON1$^{-/-}$ microglia compared to WT, but decreased with LPS treatment of both WT and PON1$^{-/-}$ microglia, similar to the results of the phagocytosis assay. Expression of the guanine nucleotide exchange factors, Vav2 (**Fig.7A, D**) and Vav3 (**Fig.7A, E**), and actin-related protein, Arp2 (**Fig.7A, F**), were increased in PON1$^{-/-}$ microglia compared to WT, but were not affected by LPS. The data suggested that PON1 deficiency enhanced phagocytosis by activation of the TREM2 signaling pathway and up-regulation of the actin cytoskeleton. As shown above, TREM2 protein

levels were significantly increased in PON1$^{-/-}$ microglia compared to WT (**Fig. 7A, B**) even though TREM2 mRNA was not altered by PON1 deficiency (**Fig. 7G**). However, when human PON1 recombinant protein was added to PON1$^{-/-}$ microglia, the protein level of TREM2 and P-DAP12 was decreased dependent on the PON1 protein concentration (**Fig. 7H-J**).

PON1 protein interacts with TREM2 and promotes its lysosome localization in microglial cells

Co-immunoprecipitation (co-IP) was employed to identify the mechanism of TREM2 regulation by PON1. The results confirmed that there was a direct interaction between endogenous PON1 and TREM2 proteins in rat brain tissues (**Fig. 8A, B**) and between over-expressed human PON1 and TREM2 proteins in BV2 cells (**Fig. 8C, D**). Immunofluorescence assays verified the co-localization of TREM2 and the lysosomal marker LAMP1 in primary microglia (**Fig. 8E**). PON1$^{-/-}$ microglia showed a highly increased, clustered distribution of TREM2 on the cell surface compared to WT. After administration of recombinant human PON1 protein, the distribution of TREM2 decreased but there was increased co-localization of TREM2 with LAMP1 in WT and PON1$^{-/-}$ microglia. APOE is a novel ligand for TREM2 [37], and we used DSS crosslinking to test whether the binding of APOE and TREM2 was disrupted by PON1. The crosslinking between APOE and TREM2 was increased in PON1$^{-/-}$ rat brain tissues relative to WT (**Fig. 8F-H**), suggesting that PON1 might compete with APOE for binding to the TREM2 receptor on microglia.

Taken together, the results suggested that PON1 interacts with TREM2 and promotes its internalization and degradation in lysosomes. Conversely, PON1 deficiency increases TREM2 and causes clustering on the surface of the microglial cells (**Fig. 8I**), which might promote TREM2 binding to APOE and phagocytosis.

PON1 deficiency facilitated microglial Aβ42 clearance in vivo

We investigated the effects of PON1 knockout or not on microglial phagocytosis or Aβ clearance in a rat model of AD produced by an intrahippocampal injection of amyloid-β1-42 (Aβ1-42) (**Fig. 9A**). The results indicated that PON1 knockout enhanced the clearance of Aβ1 –42 (**Fig. 9B, C**). Aβ1 –42 injected into the hippocampus of WT and PON1$^{-/-}$ rats induced microglial activation, proliferation, accumulation and phagocytosis, and the amount of Aβ1 –42 then gradually decreased along with the time increase (**Fig. s6 and Fig. 9D, E**). PON1 knockout significantly increased the number of microglia cells around the injection sites and Aβ1 –42 uptake of single microglia cell, finally reduced the deposit of Aβ42 inside hippocampus neurons (**Fig. s6 and Fig. 9F, G**). On another hand, PON1 knockout decreased Aβ-induced increase of cytokines including IL-1β, TNF-α, iNOS, IL-10 and IL-6 and increased the expression of Mrc-1, one receptor mediated endocytosis (**Fig. 9H**). In contrast with LPS, Aβ1 –42 injection increased the transcription of TREM2 in both WT and PON1$^{-/-}$ rats along with the time increase**,** and the protein level of TREM2 in PON1$^{-/-}$ rats was still higher than WT rats (14 days post-injection) (**Fig. s7)**. These results suggest that PON1 knockout and increased TREM2 protein level may facilitate microglial clearance of exogenic Aβ in rat brains.

Discussion

The expression of PON1 in brain has long been controversial. PON1 immunostaining showed the presence of protein in white matter areas of mouse [16] and rat brains [38], and the Human Protein Atlas program has just detected weak PON1 protein expression in human glioblastoma. PON1 mRNA was also detected in homogenates of the frontal cortex of AD and healthy controls [15], as well as in the frontal cortex of rat brain [17]. In our study, PON1 mRNA was detected in human prefrontal lobe and rat brain tissues, and PON1 protein was expressed in rat brain and microglia. Thus, it is inferred that both local synthesis and HDL delivery from liver contribute to the wide distribution of PON1 in brain [38, 39]; but its role in brain disease is unclear.

Our previous research revealed that PON1 KO impaired T cell development in rat thymus [25], suggesting that PON1 functions as a novel immune regulator. In the present study, we found that microglia from PON1 KO rats were larger in cell body and had fewer and shorter branches. PON1 KO reduced LPS-induced microglia activation (Fig. 3), promoted phagocytosis (Fig. 5) and inhibited the production of specific cytokines (Fig. 4). These data were similar to previous reports on PON1 KO mice in which macrophages were larger, contained larger cytosolic compartments, and appeared more granular than control C57BL/6 macrophages and rePON1 inhibited monocyte-to-macrophage differentiation [35]. Interestingly, we found that PON1 KO protected rats from LPS-induced lethality and decreased the LPS-induced TNF-α release in serum (Fig. 2), these data are similar to the previous data of Van Oosten et al., who showed that apolipoprotein E (APOE) protection from LPS lethality and inhibited the LPS-induced increase in TNF-α [34]. Thus, it seemed that PON1 had an opposite effect on LPS endotoxemia and on the release of TNF-α by macrophages or microglia compared to APOE. APOE has been suggested as a putative ligand for the recently identified immune receptor, TREM2, which is mainly expressed on microglia and promotes anti-inflammatory responses and phagocytosis [40–42]. APOE binding increased phagocytosis by primary microglia dependent upon TREM2 expression [37]. Our results demonstrated the interaction of PON1 with TREM2 and the up-regulation of TREM2 by PON1 KO. Thus, we proposed that PON1 might affect microglial phagocytosis by competing with APOE for binding to the TREM2 receptor on microglia (Fig. 7F-H). APOE was previously reported to bind to PON1 with high affinity and the stabile PON1 complex was involved in anti-atherogenic activity [43]. Although we found that TREM2 was cross-linked with ApoE in cortical homogenates in the absence of PON1 (Fig. 8F-H), further investigations are needed to elucidate the complicated associations of PON1, APOE and TREM2.

In this study, we focused on the role of PON1 and PON1 KO-induced microglial phagocytosis. We demonstrated for the first time that the absence of PON1 in microglia increased TREM2 protein levels, which was reversed by administration of PON1 recombinant protein, in parallel with changes in phagocytic activity. TREM2 inhibited the LPS-induced pro-inflammatory responses and its up-regulation improved cognitive impairment and pathology in a mouse model of AD [44–47]. PON1 KO showed similar effects to TREM2 on microglia, promoting phagocytosis and inhibiting the production of certain cytokines. These results suggested that PON1 regulated the activation of microglia through TREM2 signaling. We verified the interaction between TREM2 and PON1 proteins, and showed that the interaction

could promote the internalization of TREM2 into lysosomes and potential degradation, but additional research needs to be done to confirm this.

LPS triggers inflammatory responses in humans and other mammals. Many papers reported that LPS promoted phagocytosis [48–50], while some studies showed an inhibitory effect of LPS on phagocytosis [51–53]. We demonstrated that LPS significantly enhanced the production of TNF-α in microglia and inhibited PON1 KO-induced phagocytosis. Previous studies reported that TLR4 activation by LPS impaired the phagocytic capacity of microglia [51]. TNF-α inhibited phagocytosis induced by activated macrophages [52, 53], suggesting that the level of TNF-α was negatively correlated with the phagocytic ability of macrophages. LPS or PON1 down-regulated TREM2 (Fig. 6A, H), which might also be responsible for the reduction in phagocytosis seen after exposure to LPS. This result is consistent with a previous report that LPS down-regulated TREM2 mRNA in BV2 cells [54].

Conclusion

In conclusion, the present study offers evidence that upregulation of TREM2 by PON1 knockout facilitates microglial phagocytosis and inhibits the production of proinflammatory cytokines both in vivo and in vitro; the interaction between PON1 and TREM2 resulted in the localization of TREM2 to lysosomes. These findings provide insights into the role of PON1 in neuroinflammation and illustrate the potential of TREM2-directed therapeutics in neurodegenerative diseases.

Abbreviations

Aβ: Amyloid β; PON1: Paraoxonase 1; TREM2: triggering receptor expressed in myeloid cells 2; LPS: lipopolysaccharide; APOE: Apolipoprotein E ; TNF-α: Tumor necrosis factor-α; IL-1β: Interleukin-1 β; IL-6: Interleukin-6; IL-12: Interleukin-12; IL-18: Interleukin-18; IL-10: Interleukin-10; iNOS; inducible nitric oxide synthase; co-IP：Co-immunoprecipitation; KO：knockout；SDS-PAGE: dodecyl sulfate, sodium salt - Polyacrylamide gel electrophoresis, HRP: Horseradish Peroxidase; RT-PCR: Reverse Transcription-Polymerase Chain Reaction；DSS: Disuccinimidyl suberate

Declarations

Ethics approval

The experimental protocol was approved by the Animal Care and Use Committees of the Institute of Laboratory Animal Science of Peking Union Medical College.

Consent for publication

All authors read and approved the final manuscript.

Availability of data and materials

The datasets used and/or analysed during the current study are available from the corresponding author on reasonable request.

Acknowledgements

Not applicable.

Author contributions

LFZ and LZ designed the study and wrote the paper, LZ, WD, YWM, LB, CXS, XZ and JWL performed the experiments. All the authors have read and approved the final manuscript.

Fundings

The present work was supported by National Science Foundation of China（31900380，31970508）、Beijing Municipal Natural Science Foundation (7172135) and CAMS Innovation Fund for Medical Sciences （CIFMS, 2016-I2M-1-004).

Competing interests

The authors declared that there are no conflicts of interests.

Consent to participate

Not applicable.

References

1. Primo-Parmo SL, Sorenson RC, Teiber J and La Du BN (1996) The human serum paraoxonase/arylesterase gene (PON1) is one member of a multigene family, Genomics 33: 498-507.
2. Draganov DI, Teiber JF, Speelman A, Osawa Y, Sunahara R and La Du BN (2005) Human paraoxonases (PON1, PON2, and PON3) are lactonases with overlapping and distinct substrate specificities, J Lipid Res 46: 1239-47. https://doi.org/10.1194/jlr.M400511-JLR200
3. Costa LG, Giordano G, Cole TB, Marsillach J and Furlong CE (2013) Paraoxonase 1 (PON1) as a genetic determinant of susceptibility to organophosphate toxicity, Toxicology 307: 115-22. https://doi.org/10.1016/j.tox.2012.07.011
4. Rajkovic MG, Rumora L and Barisic K (2011) The paraoxonase 1, 2 and 3 in humans, Biochem Med (Zagreb) 21: 122-30.
5. Mahrooz A (2016) Pharmacological Interactions of Paraoxonase 1 (PON1): A HDL-Bound Antiatherogenic Enzyme, Curr Clin Pharmacol 11: 259-264.

6. Schrader C and Rimbach G (2011) Determinants of paraoxonase 1 status: genes, drugs and nutrition, Curr Med Chem 18: 5624-43.
7. Costa LG, Vitalone A, Cole TB and Furlong CE (2005) Modulation of paraoxonase (PON1) activity, Biochem Pharmacol 69: 541-50. https://doi.org/10.1016/j.bcp.2004.08.027
8. Leviev I, Negro F and James RW (1997) Two alleles of the human paraoxonase gene produce different amounts of mRNA. An explanation for differences in serum concentrations of paraoxonase associated with the (Leu-Met54) polymorphism, Arterioscler Thromb Vasc Biol 17: 2935-9.
9. Leviev I and James RW (2000) Promoter polymorphisms of human paraoxonase PON1 gene and serum paraoxonase activities and concentrations, Arterioscler Thromb Vasc Biol 20: 516-21.
10. Kim DS, Burt AA, Ranchalis JE, Richter RJ, Marshall JK, Eintracht JF, Rosenthal EA, Furlong CE and Jarvik GP (2012) Additional Common Polymorphisms in the PON Gene Cluster Predict PON1 Activity but Not Vascular Disease, J Lipids 2012: 476316. https://doi.org/10.1155/2012/476316
11. Soran H, Schofield JD, Liu Y and Durrington PN (2015) How HDL protects LDL against atherogenic modification: paraoxonase 1 and other dramatis personae, Curr Opin Lipidol 26: 247-56. https://doi.org/10.1097/MOL.0000000000000194
12. Kowalska K, Socha E and Milnerowicz H (2015) Review: The role of paraoxonase in cardiovascular diseases, Ann Clin Lab Sci 45: 226-33.
13. Eren E, Yilmaz N and Aydin O (2013) Functionally defective high-density lipoprotein and paraoxonase: a couple for endothelial dysfunction in atherosclerosis, Cholesterol 2013: 792090. https://doi.org/10.1155/2013/792090
14. Dahabreh IJ, Kitsios GD, Kent DM and Trikalinos TA (2010) Paraoxonase 1 polymorphisms and ischemic stroke risk: A systematic review and meta-analysis, Genet Med 12: 606-15. https://doi.org/10.1097/GIM.0b013e3181ee81c6
15. Leduc V, Legault V, Dea D and Poirier J (2011) Normalization of gene expression using SYBR green qPCR: a case for paraoxonase 1 and 2 in Alzheimer's disease brains, J Neurosci Methods 200: 14-9. https://doi.org/10.1016/j.jneumeth.2011.05.026
16. Marsillach J, Mackness B, Mackness M, Riu F, Beltran R, Joven J and Camps J (2008) Immunohistochemical analysis of paraoxonases-1, 2, and 3 expression in normal mouse tissues, Free Radic Biol Med 45: 146-57. https://doi.org/10.1016/j.freeradbiomed.2008.03.023
17. Almutairi MM, Alanazi WA, Alshammari MA, Alotaibi MR, Alhoshani AR, Al-Rejaie SS, Hafez MM and Al-Shabanah OA (2017) Neuro-protective effect of rutin against Cisplatin-induced neurotoxic rat model, BMC Complement Altern Med 17: 472. https://doi.org/10.1186/s12906-017-1976-9
18. Carmine A, Buervenich S, Sydow O, Anvret M and Olson L (2002) Further evidence for an association of the paraoxonase 1 (PON1) Met-54 allele with Parkinson's disease, Mov Disord 17: 764-6. https://doi.org/10.1002/mds.10172
19. Zintzaras E and Hadjigeorgiou GM (2004) Association of paraoxonase 1 gene polymorphisms with risk of Parkinson's disease: a meta-analysis, J Hum Genet 49: 474-81. https://doi.org/10.1007/s10038-004-0176-x

20. Leduc V and Poirier J (2008) Polymorphisms at the paraoxonase 1 L55M and Q192R loci affect the pathophysiology of Alzheimer's disease: emphasis on the cholinergic system and beta-amyloid levels, Neurodegener Dis 5: 225-7. https://doi.org/10.1159/000113709
21. Paragh G, Balla P, Katona E, Seres I, Egerhazi A and Degrell I (2002) Serum paraoxonase activity changes in patients with Alzheimer's disease and vascular dementia, Eur Arch Psychiatry Clin Neurosci 252: 63-7. https://doi.org/10.1007/s004060200013
22. Wehr H, Bednarska-Makaruk M, Graban A, Lipczynska-Lojkowska W, Rodo M, Bochynska A and Ryglewicz D (2009) Paraoxonase activity and dementia, J Neurol Sci 283: 107-8. https://doi.org/10.1016/j.jns.2009.02.317
23. Pi Y, Zhang L, Chang K, Li B, Guo L, Fang C, Gao C, Wang J, Xiang J and Li J (2012) Lack of an association between Paraoxonase 1 gene polymorphisms (Q192R, L55M) and Alzheimer's disease: a meta-analysis, Neurosci Lett 523: 174-9. https://doi.org/10.1016/j.neulet.2012.06.071
24. Wingo TS, Rosen A, Cutler DJ, Lah JJ and Levey AI (2012) Paraoxonase-1 polymorphisms in Alzheimer's disease, Parkinson's disease, and AD-PD spectrum diseases, Neurobiol Aging 33: 204 e13-5. https://doi.org/10.1016/j.neurobiolaging.2010.08.010
25. Bai L, Shi G, Ma Y, Zhang L, Guan F, Zhang X, Xu Y, Chen H and Zhang L (2018) Paraoxonase 1 knockout rats have impaired T cell development at the CD4/CD8 double-negative to double-positive transition stage, Sci Rep 8: 14457. https://doi.org/10.1038/s41598-018-32780-w
26. Wolf SA, Boddeke HW and Kettenmann H (2017) Microglia in Physiology and Disease, Annu Rev Physiol 79: 619-643. https://doi.org/10.1146/annurev-physiol-022516-034406
27. Sasaki A (2017) Microglia and brain macrophages: An update, Neuropathology 37: 452-464. https://doi.org/10.1111/neup.12354
28. Zhang L, Sun C, Jin Y, Gao K, Shi X, Qiu W, Ma C and Zhang L (2017) Dickkopf 3 (Dkk3) Improves Amyloid-beta Pathology, Cognitive Dysfunction, and Cerebral Glucose Metabolism in a Transgenic Mouse Model of Alzheimer's Disease, J Alzheimers Dis 60: 733-746. https://doi.org/10.3233/JAD-161254
29. Young K and Morrison H (2018) Quantifying Microglia Morphology from Photomicrographs of Immunohistochemistry Prepared Tissue Using ImageJ, J Vis Exp. https://doi.org/10.3791/57648
30. Tamashiro TT, Dalgard CL and Byrnes KR (2012) Primary microglia isolation from mixed glial cell cultures of neonatal rat brain tissue, J Vis Exp: e3814. https://doi.org/10.3791/3814
31. Chernyavskiy I, Veeranki S, Sen U and Tyagi SC (2016) Atherogenesis: hyperhomocysteinemia interactions with LDL, macrophage function, paraoxonase 1, and exercise, Ann N Y Acad Sci 1363: 138-54. https://doi.org/10.1111/nyas.13009
32. Galanos C, Freudenberg MA and Reutter W (1979) Galactosamine-induced sensitization to the lethal effects of endotoxin, Proc Natl Acad Sci U S A 76: 5939-43. https://doi.org/10.1073/pnas.76.11.5939
33. Endo Y, Shibazaki M, Yamaguchi K, Kai K, Sugawara S, Takada H, Kikuchi H and Kumagai K (1999) Enhancement by galactosamine of lipopolysaccharide(LPS)-induced tumour necrosis factor

production and lethality: its suppression by LPS pretreatment, Br J Pharmacol 128: 5-12. https://doi.org/10.1038/sj.bjp.0702747

34. Van Oosten M, Rensen PC, Van Amersfoort ES, Van Eck M, Van Dam AM, Breve JJ, Vogel T, Panet A, Van Berkel TJ and Kuiper J (2001) Apolipoprotein E protects against bacterial lipopolysaccharide-induced lethality. A new therapeutic approach to treat gram-negative sepsis, J Biol Chem 276: 8820-4. https://doi.org/10.1074/jbc.M009915200
35. Rosenblat M, Volkova N, Ward J and Aviram M (2011) Paraoxonase 1 (PON1) inhibits monocyte-to-macrophage differentiation, Atherosclerosis 219: 49-56. https://doi.org/10.1016/j.atherosclerosis.2011.06.054
36. Paresce DM, Ghosh RN and Maxfield FR (1996) Microglial cells internalize aggregates of the Alzheimer's disease amyloid beta-protein via a scavenger receptor, Neuron 17: 553-65. https://doi.org/10.1016/s0896-6273(00)80187-7
37. Atagi Y, Liu CC, Painter MM, Chen XF, Verbeeck C, Zheng H, Li X, Rademakers R, Kang SS, Xu H, Younkin S, Das P, Fryer JD and Bu G (2015) Apolipoprotein E Is a Ligand for Triggering Receptor Expressed on Myeloid Cells 2 (TREM2), J Biol Chem 290: 26043-50. https://doi.org/10.1074/jbc.M115.679043
38. Rodrigo L, Hernandez AF, Lopez-Caballero JJ, Gil F and Pla A (2001) Immunohistochemical evidence for the expression and induction of paraoxonase in rat liver, kidney, lung and brain tissue. Implications for its physiological role, Chem Biol Interact 137: 123-37. https://doi.org/10.1016/s0009-2797(01)00225-3
39. Mackness B, Beltran-Debon R, Aragones G, Joven J, Camps J and Mackness M (2010) Human tissue distribution of paraoxonases 1 and 2 mRNA, IUBMB Life 62: 480-2. https://doi.org/10.1002/iub.347
40. Zhai Q, Li F, Chen X, Jia J, Sun S, Zhou D, Ma L, Jiang T, Bai F, Xiong L and Wang Q (2017) Triggering Receptor Expressed on Myeloid Cells 2, a Novel Regulator of Immunocyte Phenotypes, Confers Neuroprotection by Relieving Neuroinflammation, Anesthesiology 127: 98-110. https://doi.org/10.1097/ALN.0000000000001628
41. Lee CYD, Daggett A, Gu X, Jiang LL, Langfelder P, Li X, Wang N, Zhao Y, Park CS, Cooper Y, Ferando I, Mody I, Coppola G, Xu H and Yang XW (2018) Elevated TREM2 Gene Dosage Reprograms Microglia Responsivity and Ameliorates Pathological Phenotypes in Alzheimer's Disease Models, Neuron 97: 1032-1048 e5. https://doi.org/10.1016/j.neuron.2018.02.002
42. Wolfe CM, Fitz NF, Nam KN, Lefterov I and Koldamova R (2018) The Role of APOE and TREM2 in Alzheimer's Disease-Current Understanding and Perspectives, Int J Mol Sci 20. https://doi.org/10.3390/ijms20010081
43. Gaidukov L, Viji RI, Yacobson S, Rosenblat M, Aviram M and Tawfik DS (2010) ApoE induces serum paraoxonase PON1 activity and stability similar to ApoA-I, Biochemistry 49: 532-8. https://doi.org/10.1021/bi9013227
44. Painter MM, Atagi Y, Liu CC, Rademakers R, Xu H, Fryer JD and Bu G (2015) TREM2 in CNS homeostasis and neurodegenerative disease, Mol Neurodegener 10: 43.

https://doi.org/10.1186/s13024-015-0040-9

45. Zhong L, Chen XF, Zhang ZL, Wang Z, Shi XZ, Xu K, Zhang YW, Xu H and Bu G (2015) DAP12 Stabilizes the C-terminal Fragment of the Triggering Receptor Expressed on Myeloid Cells-2 (TREM2) and Protects against LPS-induced Pro-inflammatory Response, J Biol Chem 290: 15866-77. https://doi.org/10.1074/jbc.M115.645986
46. Jiang T, Tan L, Zhu XC, Zhang QQ, Cao L, Tan MS, Gu LZ, Wang HF, Ding ZZ, Zhang YD and Yu JT (2014) Upregulation of TREM2 ameliorates neuropathology and rescues spatial cognitive impairment in a transgenic mouse model of Alzheimer's disease, Neuropsychopharmacology 39: 2949-62. https://doi.org/10.1038/npp.2014.164
47. Jay TR, von Saucken VE and Landreth GE (2017) TREM2 in Neurodegenerative Diseases, Mol Neurodegener 12: 56. https://doi.org/10.1186/s13024-017-0197-5
48. Kobayashi Y, Inagawa H, Kohchi C, Okazaki K, Zhang R, Kobara H, Masaki T and Soma GI (2017) Lipopolysaccharides Derived from Pantoea agglomerans Can Promote the Phagocytic Activity of Amyloid beta in Mouse Microglial Cells, Anticancer Res 37: 3917-3920. https://doi.org/10.21873/anticanres.11774
49. Inagawa H, Kobayashi Y, Kohchi C, Zhang R, Shibasaki Y and Soma G (2016) Primed Activation of Macrophages by Oral Administration of Lipopolysaccharide Derived from Pantoea agglomerans, In Vivo 30: 205-11.
50. Fricker M, Oliva-Martin MJ and Brown GC (2012) Primary phagocytosis of viable neurons by microglia activated with LPS or Abeta is dependent on calreticulin/LRP phagocytic signalling, J Neuroinflammation 9: 196. https://doi.org/10.1186/1742-2094-9-196
51. Lee JW, Nam H, Kim LE, Jeon Y, Min H, Ha S, Lee Y, Kim SY, Lee SJ, Kim EK and Yu SW (2019) TLR4 (toll-like receptor 4) activation suppresses autophagy through inhibition of FOXO3 and impairs phagocytic capacity of microglia, Autophagy 15: 753-770. https://doi.org/10.1080/15548627.2018.1556946
52. Feng X, Deng T, Zhang Y, Su S, Wei C and Han D (2011) Lipopolysaccharide inhibits macrophage phagocytosis of apoptotic neutrophils by regulating the production of tumour necrosis factor alpha and growth arrest-specific gene 6, Immunology 132: 287-95. https://doi.org/10.1111/j.1365-2567.2010.03364.x
53. Li X, Darby J, Lyons AB, Woods GM and Korner H (2019) TNF May Negatively Regulate Phagocytosis of Devil Facial Tumour Disease Cells by Activated Macrophages, Immunol Invest 48: 691-703. https://doi.org/10.1080/08820139.2018.1515222
54. Zhong L, Zhang ZL, Li X, Liao C, Mou P, Wang T, Wang Z, Wang Z, Wei M, Xu H, Bu G and Chen XF (2017) TREM2/DAP12 Complex Regulates Inflammatory Responses in Microglia via the JNK Signaling Pathway, Front Aging Neurosci 9: 204. https://doi.org/10.3389/fnagi.2017.00204

Tables

Table 1. Significantly enriched GO terms (biological process) affected by PON1 knockout or in combination with LPS treatment.

PON1$^{-/-}$ vs WT					
Factor	DAVID	Go terms	Down-reg genes	up-reg genes	*p* value
PON1 KO	GO:0007399	nervous system development	*n* =46	*n* =2	5.05E-08
	GO:0007267	cell-cell signaling	*n* =26	*n* =0	2.75E-05
	Go:0010001	glial cell differentiation	*n* =11	*n* =0	6.94E-06
	Go:0042063	gliogenesis	*n* =12	*n* =0	1.02E-05
PON1$^{-/-}$ LPS vs WT LPS					
Factor	DAVID	Go terms	Down-reg genes	up-reg genes	*p* value
PON1 KO and LPS treatment	GO:0007399	nervous system development	*n* = 47	*n* =7	3.77E-09
	GO:0007267	cell-cell signaling	*n* =25	*n* =4	1.07E-05
	Go:0010001	glial cell differentiation	*n* =14	*n* =0	8.58E-08
	Go:0042063	gliogenesis	*n* =14	*n* =0	1.22E-06
	GO:0035637	regulation of ion transport	*n* =16	*n* =3	2.99E-05

Abbreviations: DAVID, database for annotation, visualization and integrated discovery; GO, gene ontology; KO, knockout; up-reg, up-regulated; down-reg, down-regulated.

Figures

Fig.1

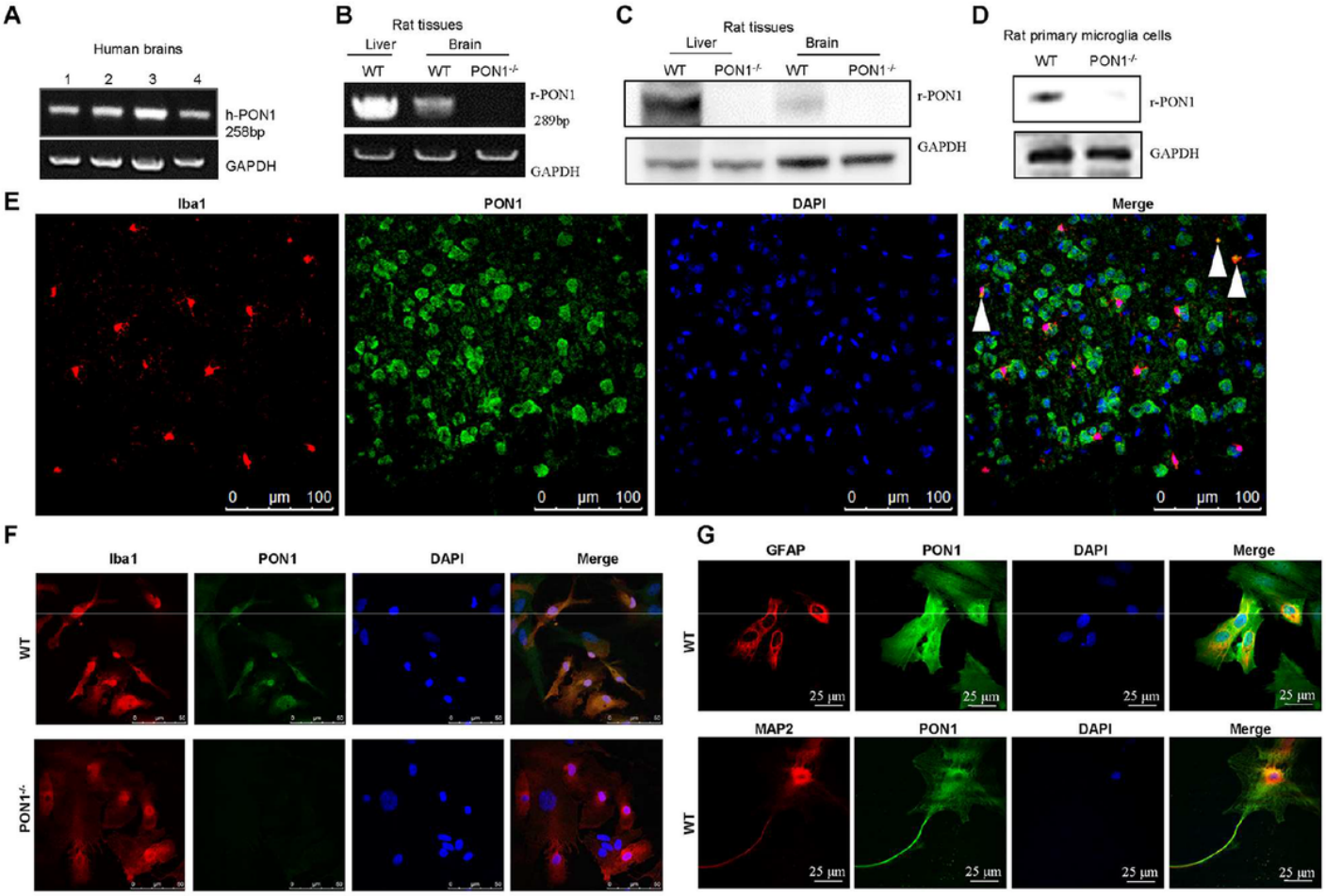

Figure 1

Expression of PON1 in brain tissues and rat primary microglia. PON1 mRNA was detected in brain tissues (A) from control human postmortem samples (n = 4) or liver and brain tissues (B) from wild type rat (WT, n = 3) and PON1 KO rat (PON1-/-, n = 3) by RT-PCR. The absence of PON1 mRNA in PON1-/- rat was verified. The expression of PON1 protein in liver and brain tissues (C) from WT rats (n = 3) and PON1-/- rats (n = 3) or in primary microglia (D) isolated from three day-old WT rats (n = 3) and PON1-/- rats (n = 3) was compared by western blot. Double immunofluorescence staining of microglia using antibody against PON1 (green) and Iba1 (red) were performed on brain sections (E) of WT rats (n = 4, magnification ×200, scale bar = 100 μm, arrows indicate co-localization) or in primary microglia (F) isolated from WT and PON1-/- rat (n = 4 each group, magnification ×630, scale bar = 50 μm). (G) Double immunofluorescence staining of PON1 (green) and MAP2 (red) or of PON1 (green) and GFAP (red) were done in primary neurons or astrocytes from WT rats (n = 6, magnification ×630, scale bar = 25 μm). The nuclei were stained using DAPI (blue).

Fig.2

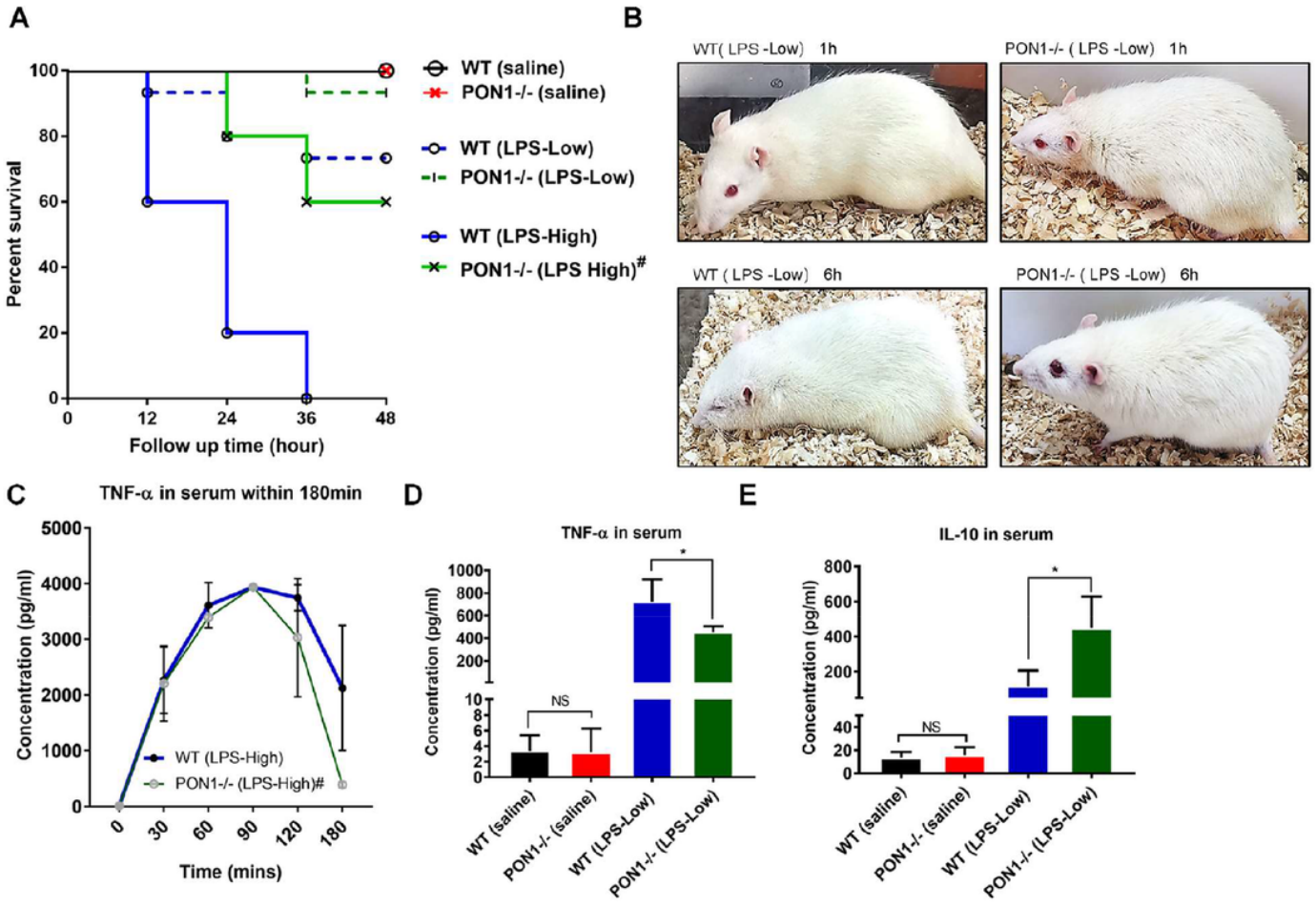

Figure 2

PON1 deficiency and LPS-induced lethality. WT and PON1-/- rats were injected intraperitoneally with saline or LPS (n = 8 or 7 for saline-treated group named WT (saline) and PON1-/- (saline); n =15 per group for the 5 mg/kg LPS treatment group named WT (LPS-Low) and PON1-/- (LPS-Low); n =5 per group for the 20 mg/kg LPS treatment group named WT (LPS-High) and PON1-/- (LPS-High)). (A) Kaplan-Meier survival curve. # p<0.05 PON1-/- (LPS-High) versus WT (LPS-High). (B) Representative images of WT (LPS-Low) and PON1-/- (LPS-Low) rats 1h or 6h post-injection. At the indicated time points, blood samples were taken and serum TNF-α levels in (C) of WT (saline), PON1-/-(saline), WT (LPS-High) and PON1-/- (LPS-High) rats were determined by ELISA (n = 4/group, male). Data indicate the mean± SD. # p<0.05 PON1-/- (LPS-High) versus WT (LPS-High). TNF-α level (D) and IL-10 level (E) of WT (saline), PON1-/- (saline), WT (LPS-Low) and PON1-/- (LPS-Low) rats 6 h post-injection of 5 mg/kg LPS were also determined by ELISA (n = 4/group). Data are the mean± SD. * p<0.05 PON1-/- (LPS-Low) versus WT (LPS-Low). NS indicates no significance, PON1-/-(saline) versus WT (saline).

Fig.3

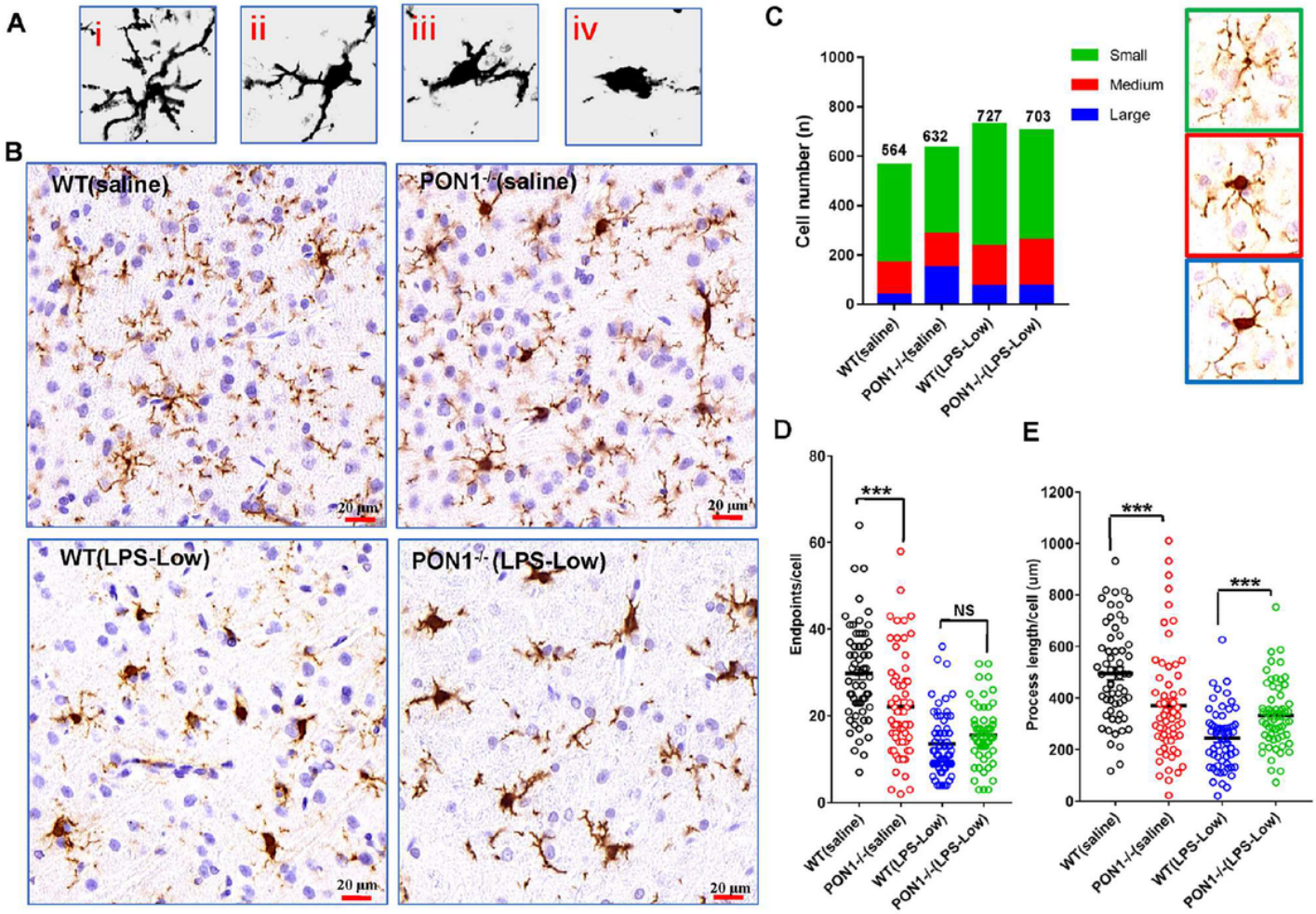

Figure 3

Effect of PON1 loss on LPS-induced morphological changes in microglia in rat brain sections. (A) Representative micrographs of single microglia stained for Iba-1 show morphological evolution from resting to active phenotype. (i) ramified microglial cells with projections; (ii) cells with short projections and enlarged bodies; (iii) hypertrophic cells; and (iv) amoeboid cells; (B) Representative images of Iba1-labeled microglia in brain sections of WT (saline), PON1-/- (saline), WT (LPS-Low) and PON1-/- (LPS-Low) rats. (C) Five serial brain sections from each rat were used to count the number of Iba 1-labeled microglia and three types of Iba1-positive cells with small, medium and large cell bodies were counted, quantified and compared (mean ± SEM, n = 6 rats per group). Quantification of the number of projections (D) and lengths of projections (E) of microglia were performed using Image J (sixty cells from 6 rats for each group). ***p<0.001 indicates significance; NS indicates no significance.

Fig.4

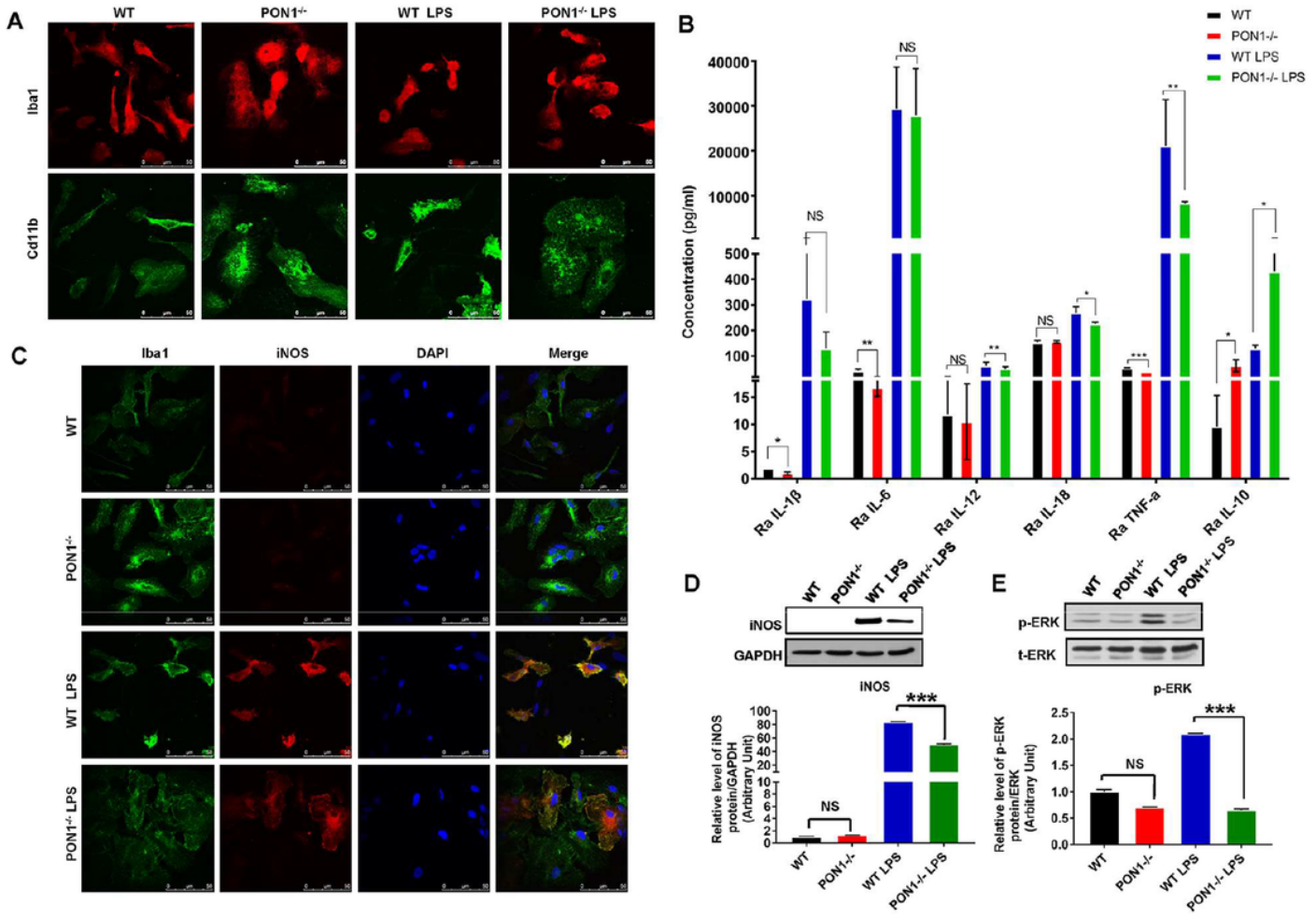

Figure 4

Effect of PON1 loss on LPS-induced changes in morphology and cytokine production in rat primary microglia. Microglia isolated from WT and PON1-/- rats (n = 9 rats per group) were treated with 200 ng/mL LPS or PBS for 24 h (WT, PON1-/-, WT LPS, PON1-/- LPS). (A) Staining of Iba1 (red) and Cd11b (green) was performed and immunofluorescence was observed by confocal microscopy (magnification ×630, scale bar = 50 μm). (B)The levels of IL-1β, IL-6, IL-12, IL-18, TNF-α and IL-10 in cell supernatants (n = 3 samples per group) were measured using a 23-plex rat cytokine panel. (C) Double immunofluorescence label staining of Cd11b (green) and iNOS (red) was performed in WT, PON1-/-, WT LPS and PON1-/- LPS microglia (magnification ×630, scale bar = 50 μm). Total protein lysates of WT, PON1-/-, WT LPS and PON1-/- LPS microglia were collected and iNOS (D), P-ERK and ERK (E) were detected by western blot. Quantitative analysis of iNOS using GAPDH (D) and P-ERK using t-ERK (E) for

normalization were performed by Image J. The nuclei were stained with DAPI (blue). * p<0.05, ** p<0.01, and *** p<0.001 indicate significance; NS indicates no significance.

Fig.5

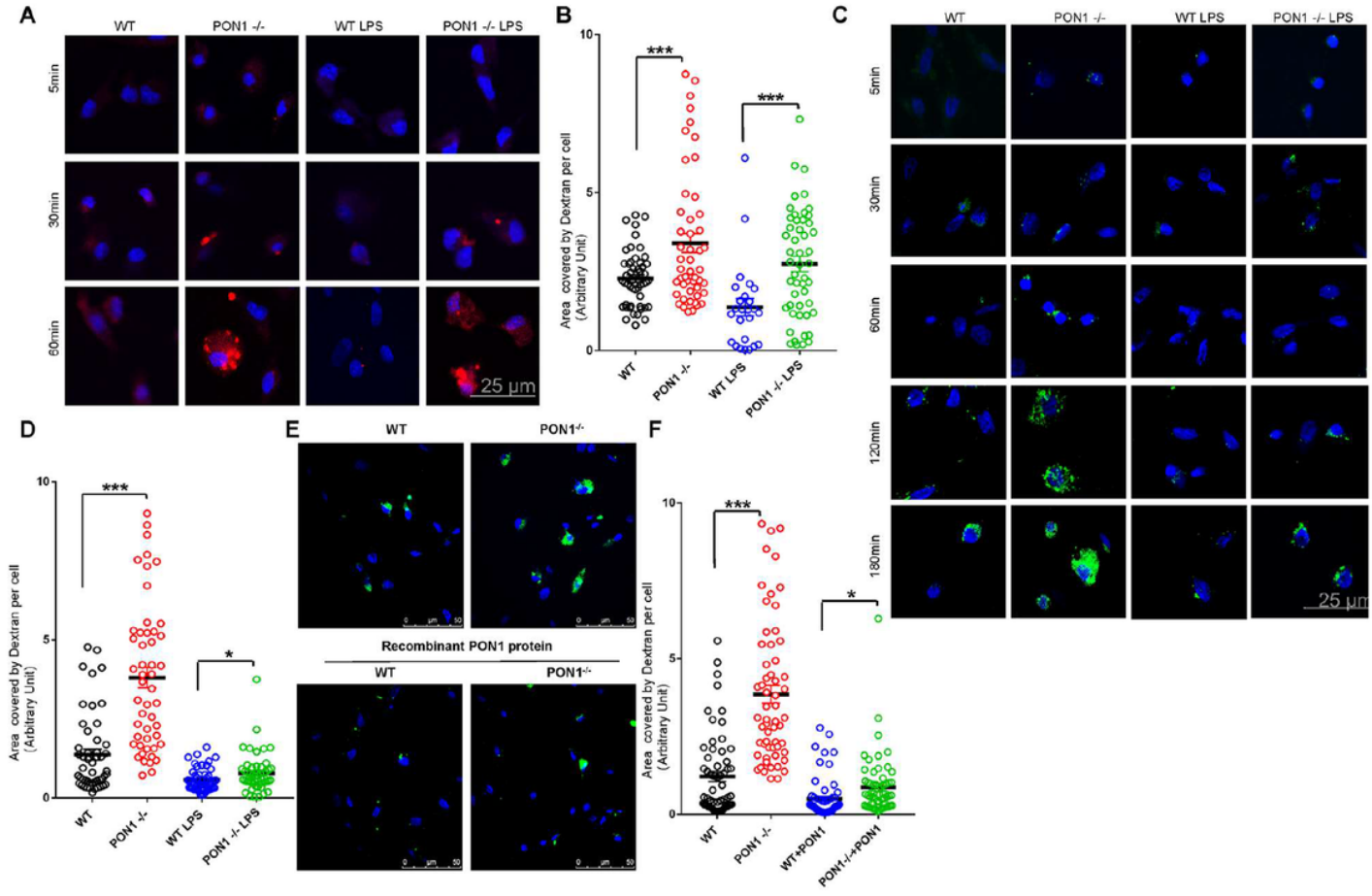

Figure 5

PON1 deficiency enhances microglial phagocytosis Primary microglia isolated from WT and PON1-/- rats (n = 12 rats per group) were treated with 200 ng/mL LPS or PBS for 24 h (WT, PON1-/-, WT LPS, PON1-/- LPS). Microglial phagocytosis of TAMRA-labeled amyloid (A) or FITC-dextran (C) was observed under confocal microscopy at the indicated time points and areas covered by Aβ for 1h (B, fifty cells per group except 25 cells for WT LPS group) or dextran for 3h (D, fifty cells per group) of were quantified using Image J (magnification ×630, zoom 2, scale bar = 25 μm). Primary microglia isolated from WT and PON1-/- rats (n = 6 rats per group) were exposed to human recombinant PON1 protein at a concentration of 1ng/ul or PBS for 1 h (WT, PON1-/-, WT+PON1, PON1-/-+PON1). The microglial phagocytosis of FITC-dextran for 3 h was observed under confocal microscopy (magnification ×630, scale bar = 50 μm) (E) and areas covered by dextran were quantified (F, sixty cells per group) using image J. The nuclei were stained with DAPI (blue). * p<0.05, ** p<0.01, and *** p<0.001 indicate significance.

Fig.6

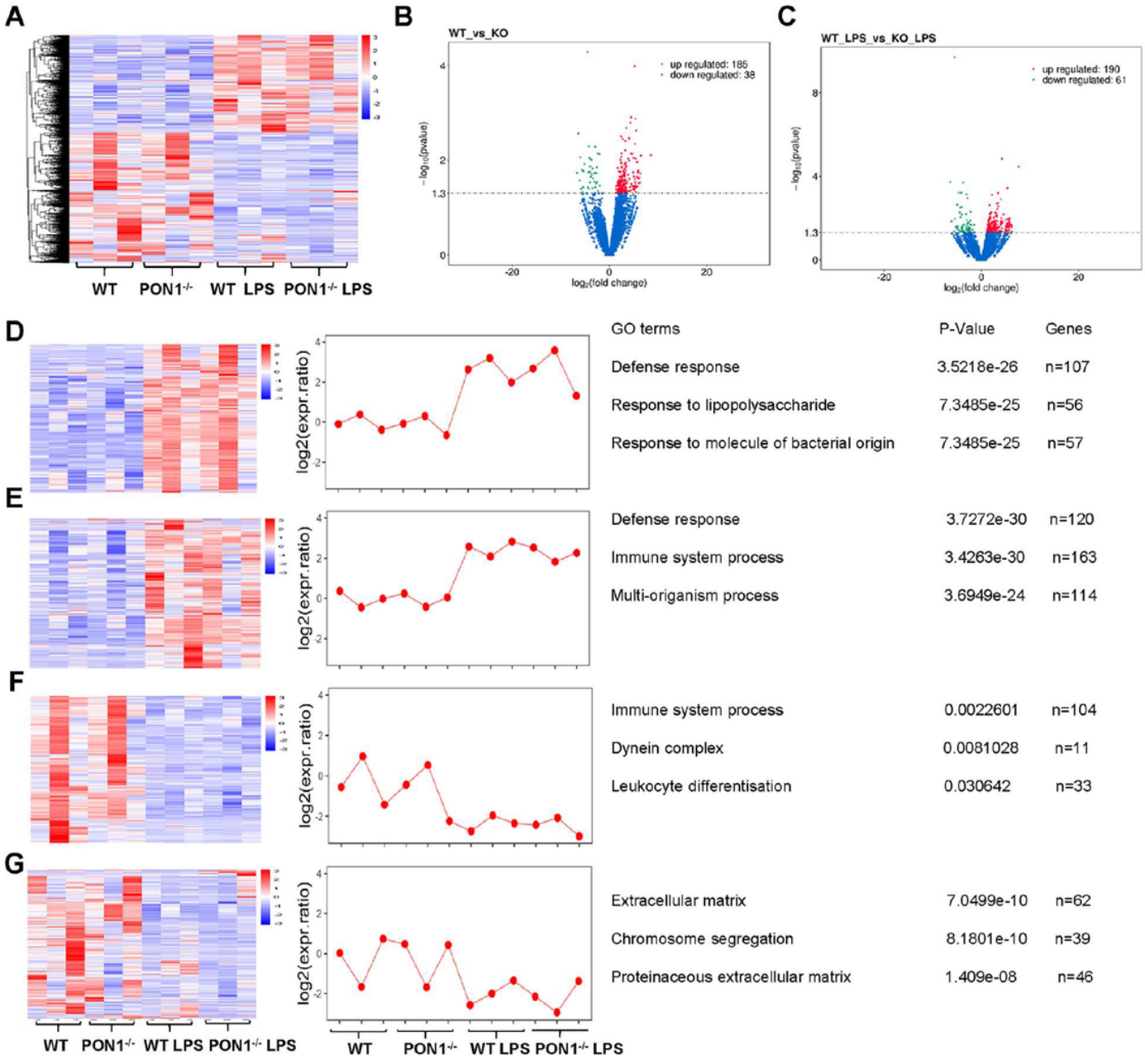

Figure 6

Comparison of transcriptome profiles in rat primary microglia. (A) The integrated heat map showed differential gene expression in WT, PON1-/-, WT LPS and PON1-/- LPS microglia (n=3 cell samples from 9 rats each group). Volcano plots depict the genes differentially expressed between WT and PON1-/- microglia (B) and between WT LPS and PON1-/- LPS microglia (C). Differentially expressed genes were classified into four categories using the SOTA function in the clValid package. Among them, two categories of genes were significantly up-regulated (D and E) and two categories were significantly down-regulated (F and G) in LPS-treated WT and PON1-/- microglia compared to controls. The top GO terms, corresponding to enrichment p values and gene numbers are shown on the right side.

Fig.7

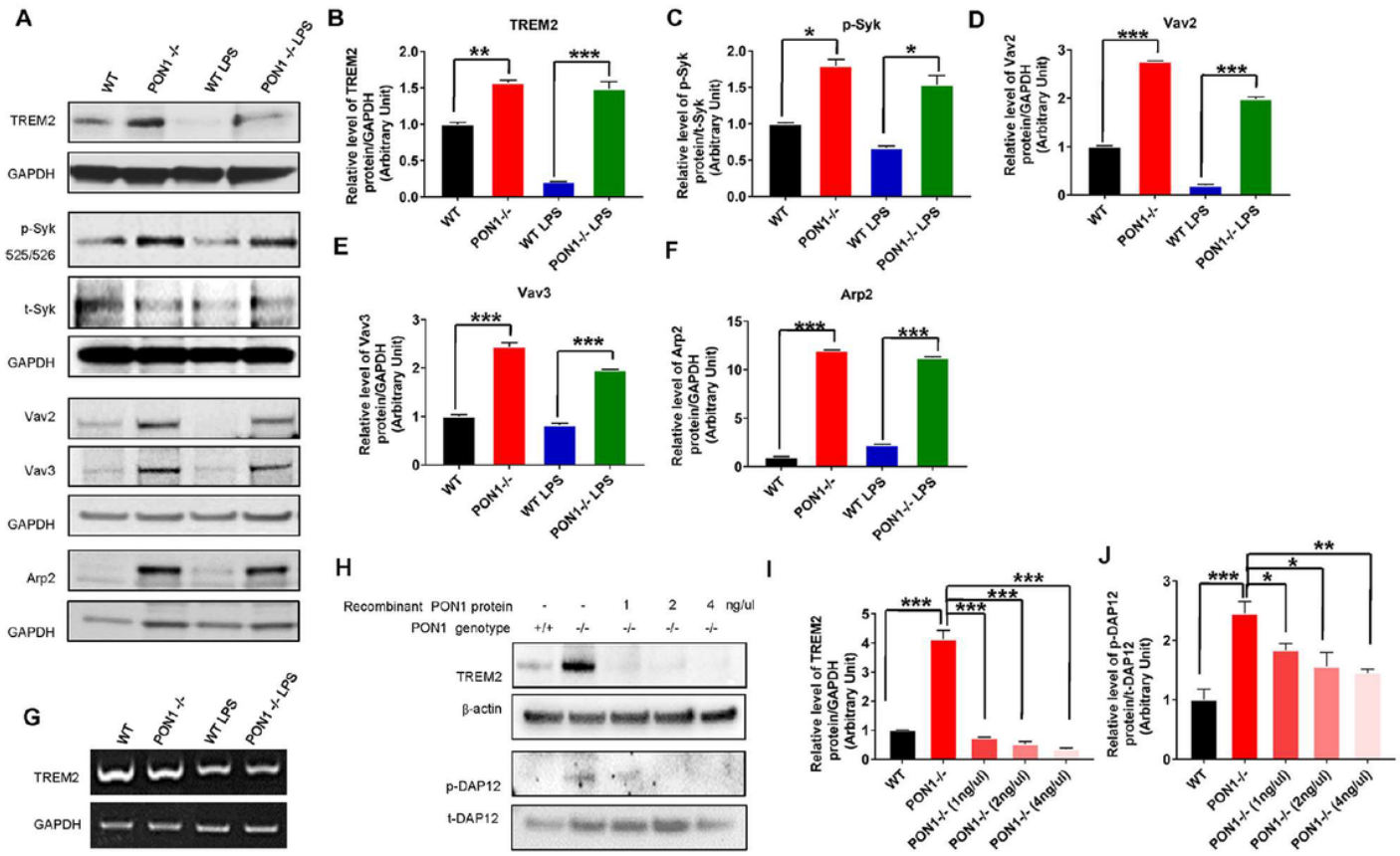

Figure 7

PON1 deficiency activates TREM2 signaling in rat primary microglia. The total protein lysates of WT, PON1-/-, WT LPS and PON1-/- LPS microglia were prepared and the levels of TREM2 (A and B), P-Syk (A and C), Vav2 (A and D), Vav3 (A and E) and Arp2 (A and F) were determined by western immunoblotting. The relative protein expression levels of TREM2, Vav2, Vav3, and Arp2 were normalized to GAPDH and the relative protein expression of P-Syk was normalized to t-Syk. Values are expressed as mean ± S.D. (n = 3 each group). (G) Total RNA from WT, PON1-/-, WT LPS and PON1-/- LPS microglia was isolated and the mRNA level of TREM2 was determined by RT-PCR with GAPDH used for normalization. Total protein lysates from WT and PON1-/- microglia incubated with recombinant PON1 protein for 24h at a concentration of 0, 1, 2, 4 ng/ul were prepared and the level of TREM2 (H and I) and P-DAP12 (H and J) were determined by western blot. The relative protein expression levels of TREM2 were normalized to β-actin and the relative protein expression of P- DAP12 was normalized to t- DAP12. Values are expressed as mean ± S.D. (n = 3).* p<0.05, ** p <0.01, *** p<0.001 indicate significance.

Fig.8

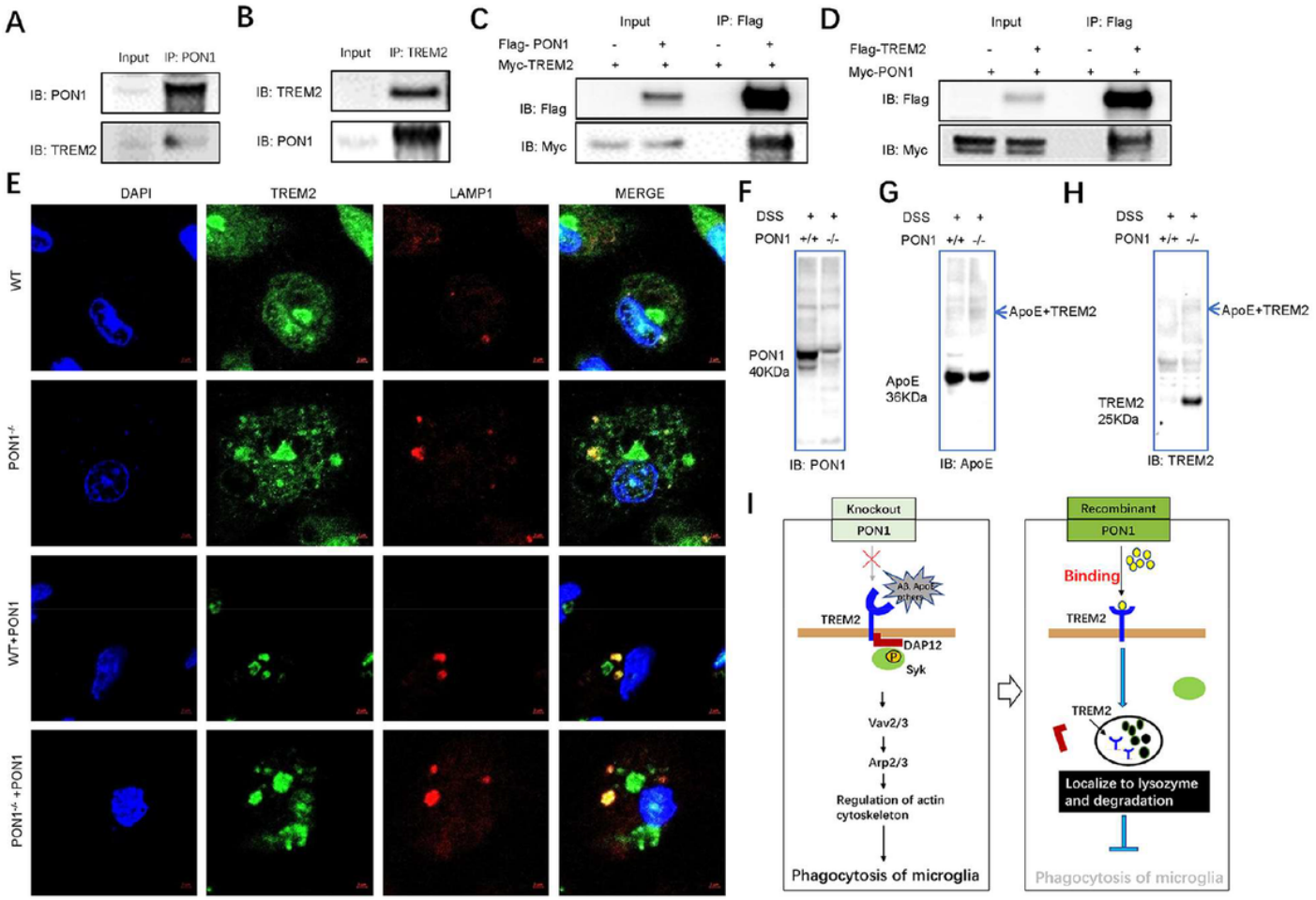

Figure 8

Interaction between PON1 and TREM2. Co-immunoprecipitation (Co-IP) was used to determine the interaction between TREM2 and PON1 in WT rat brains and BV2 cells over-expressing PON1. Western blots showed co-IP of endogenous PON1 and TREM2 by anti- PON1 antibody (A) or by anti-TREM2 antibody (B) in rat brain tissues (n =6). Flag-PON1 or empty vector was co-transfected with Myc-TREM2 into 1.0 × 107 BV2 cells. The tags were then switched (Flag-TREM2 and Myc-PON1) and the co-transfection repeated. BV2 lysates were immunoprecipitated with anti-FLAG M2 beads and western blots showed co-IP of PON1 and TREM2 (C and D). Next, WT and PON1-/- microglia were incubated with 1ng/ul human PON1 recombinant protein for 15mins and immunofluorescence staining was performed to determine the distribution of TREM2 and the co-localization of TREM2 and LAMP1 proteins (E). DAPI was used to stain cell nuclei. (4× zoom of ×630 original magnification, scale bar = 2 μm). DSS crosslinking was performed on mechanically fractured rat brain tissues, and western blotting was used to detect PON1 (F), APOE (G) and TREM2 (H) proteins in control and cross-linked samples. A preliminary model of the proposed mechanism of PON1 action in microglia is shown (I).

Fig.9

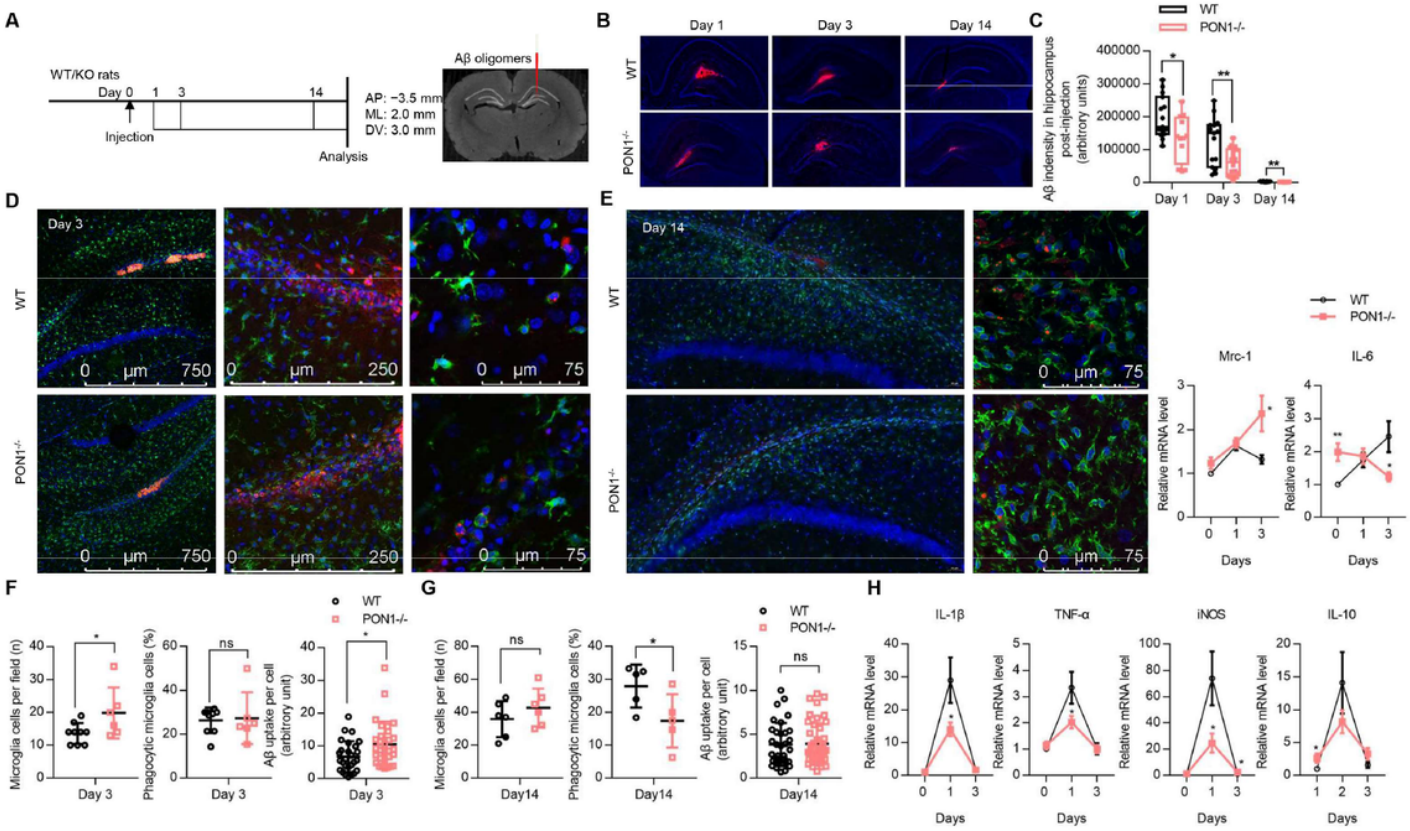

Figure 9

PON1 deficiency and Aβ clearance in vitro The protocol for Aβ injection into the hippocampus of WT and PON1-/- rats (A). Representative images (B) and quantitation analysis (C) of Aβ oligomers (red) at the injection sites of WT and PON1-/- rat brains (three sections for each rat, n= 5 WT, n= 4-6 PON1-/-). DAPI (blue) stained the nucleus. Representative confocal images (D&E) and relative quantitation analysis (F&G) of microglia labelled with Iba1 (green) merged with Aβ (red) at the injection sites of WT and PON1-/- rats 3- or 14-day post-injection. Scale bar, 750 or 250 or 50 μm. n= 9 WT, n= 6 PON1-/- for microglia cells per field and phagocytic microglia cells of Day3; n= 27 WT, n= 30 PON1-/- for Aβ uptake per cell of Day3; n= 6 WT, n= 6 PON1-/- for microglia cells per field of Day14; n= 5 WT, n= 5 PON1-/- for phagocytic microglia cells of Day14; n= 33 WT, n= 45 PON1-/- for Aβ uptake per cell of Day14. The relative mRNA levels of IL-1β, TNF-α, iNOS, IL-10, Mrc-1 and IL-6 in the hippocampus from WT and PON1-/- rats were detected by real time PCR, and GAPDH was used for normalization (H). n= 6 for WT and PON1-/- rats 0-day post-injection; n= 4 for WT and PON1-/- rats 1-day and 3-day post-injection. * p<0.05, ** p <0.01 indicate significance, ns indicate no significance.

Supplementary Files

This is a list of supplementary files associated with this preprint. Click to download.

- Tables1andtables2.docx
- fig.s17.pdf
- figurelegendsforfig.s1s7.docx